

Properties of strained (In, Ga, Al)As lasers with laterally modulated active region

N. N. Ledentsov^{a)} and D. Bimberg

Institut für Festkörperphysik, Technische Universität Berlin, D-10623 Berlin, Germany

Yu. M. Shernyakov, V. Kochnev, M. V. Maximov, A. V. Sakharov, I. L. Krestnikov, A. Yu. Egorov, A. E. Zhukov, A. F. Tsatsul'nikov, B. V. Volovik, V. M. Ustinov, P. S. Kop'ev, and Zh. I. Alferov

A. F. Ioffe Physical-Technical Institute, Politeknicheskaya 26, 194021 Saint Petersburg, Russia

A. O. Kosogov^{a),b)} and P. Werner

Max-Planck-Institut für Mikrostrukturphysik, Weinberg 2, D-06120 Halle, Germany

(Received 19 August 1996; accepted for publication 10 February 1997)

Transmission electron microscopy studies of low indium composition $\text{In}_x\text{Ga}_{1-x}\text{As}$ insertions ($x < 0.4$) in a GaAs matrix deposited by molecular beam epitaxy or by metal-organic chemical vapor deposition reveal nanoscale quasiperiodic compositional and morphological modulations. The luminescence peak wavelength is found to be a strong function of deposition parameters and can be tuned from 1.1 to 1.3 μm for the same x and average thickness of the deposit. Strained (In, Ga, Al)As lasers with such a laterally modulated $\text{In}_x\text{Ga}_{1-x}\text{As}$ active region demonstrate significant depolarization of the electroluminescence. For short cavity length, lasing occurs at energies corresponding to transitions between $\text{In}_x\text{Ga}_{1-x}\text{As}$ conduction band and light holelike valence band states. Devices lase at low threshold current densities and demonstrate continuous wave operation up to 3 W at room temperature. © 1997 American Institute of Physics. [S0003-6951(97)02015-9]

Strong improvements in device characteristics are expected for heterostructure lasers with quantum wires (QWVs) and quantum dots (QDs) in the active region.¹ *In situ* fabrication of QWVs and QDs is possible by using spontaneous ordering effects in epitaxial films² and on crystal surfaces.³⁻⁵ It was shown, for example, that heteroepitaxy in lattice mismatched systems can result in the formation of coherent *three-dimensional* (3D) islands arranged in some cases in laterally ordered arrays.⁶ QD lasers⁷ have been fabricated using this approach and lasing via the QD ground state up to room temperature has been demonstrated.^{8,9} In most cases, materials having high lattice mismatch with the substrate were used for QD fabrication.³⁻⁹

In this letter, we study structural and luminescence properties of low indium composition ($x < 0.4$) $\text{In}_x\text{Ga}_{1-x}\text{As}$ insertions in a GaAs matrix. We show that, under particular growth conditions, pronounced quasiperiodic lateral modulations (LM) in composition and thickness occur. The resulting structures can be considered as arrays of QDs in view of the characteristic sizes involved.

The molecular beam epitaxy (MBE) samples are grown using a Riber 32 MBE machine. Details on the growth of buffer and cap layers are given in Ref. 9. $\text{In}_x\text{Ga}_{1-x}\text{As}$ regions are grown at 490 °C. These regions in samples A and B are grown using InAs and GaAs submonolayer growth cycles.¹⁰ Fifteen cycles of alternate 1 Å InAs and 1.7 Å GaAs depositions or 28 cycles of 0.75 Å InAs and 1.7 Å GaAs depositions are carried out, resulting nominally in a 41-Å-thick $\text{In}_{0.37}\text{Ga}_{0.63}\text{As}$ layer for sample A and a 69-Å-thick $\text{In}_{0.31}\text{Ga}_{0.69}\text{As}$ layer for sample B, respectively. For sample B*, the deposition sequence is similar to that of the

sample B, but the deposition of In and As and of Ga and As was performed in an alternate mode^{11,12} and the number of deposition cycles was 25.

The sample C was grown by metal-organic chemical vapor deposition (MOCVD) at 76 Torr total reactor pressure with TMGa, TMAI, EDMIn and pure AsH_3 as precursors. Hydrogen was used as a carrier gas and the V/III flux ratio was 75. After deposition of a 0.5- μm -thick buffer layer at 600 °C the substrate temperature was reduced to 490 °C and

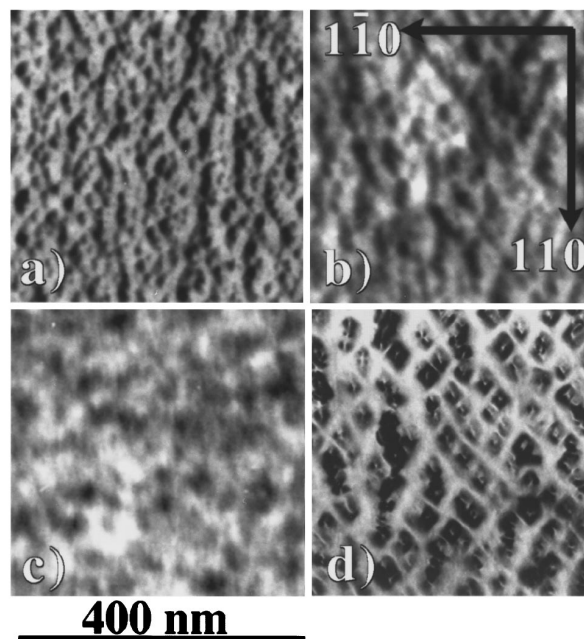


FIG. 1. (022) bright field TEM images of quantum dots formed by 15 cycles of alternate 1 Å InAs and 1.7 Å GaAs depositions (a) and by 28 cycles of 0.75 Å InAs and 1.7 Å GaAs depositions (b) TEM images of nominal 70 Å of $\text{In}_{0.2}\text{Ga}_{0.8}\text{As}$ insertion formed by MOCVD (c) and quantum dots formed by the deposition sequence similar to that of Fig. (b) but using alternate In and As and Ga and As deposition cycles (d) taken under [001] illumination

^{a)}On leave from A. F. Ioffe Physical-Technical Institute, St. Petersburg, Russia.

^{b)}Also at Institut für Festkörperphysik, TU-Berlin; Electronic mail: AOKOS@miraculix.mpi-mp-halle.mpg.de

70 Å of $\text{In}_{0.2}\text{Ga}_{0.8}\text{As}$ was deposited. After this 100 Å of GaAs was grown before the substrate temperature was increased to 600 °C to grow cap layers.

Transmission electron microscopy (TEM) investigations were performed in a JEM1000 microscope at 1 MV. Photoluminescence (PL) is excited by using the 514.5 nm line of a Ar^+ laser and detected by using a cooled germanium *pin* photodetector.

In Fig. 1(a), we show a plan-view TEM image of sample A. A dense array of InGaAs QDs in a GaAs matrix with a characteristic lateral size of about 150 Å is revealed in the image. The dots are ordered in chains along the [0–11] direction similar to ones previously reported for dots formed by $\text{In}_{0.5}\text{Ga}_{0.5}\text{As}$ deposition.¹³ Reduction in the average In composition and increase in the average $\text{In}_x\text{Ga}_{1-x}\text{As}$ thickness results in a similar arrangement except for some increase in the characteristic dot size, as it is shown in Fig. 1(b) for the sample B. The PL peak wavelength at 300 K in this case is about 1.16 μm.

A plan-view polar¹³ TEM image of the (In,Ga)As insertion formed by MOCVD is shown in Fig. 1(c). The TEM contrast represents a superposition of two lateral arrangements: stripes having approximately 50–70 Å width and oriented along the [0–11] direction, and granular structure with a characteristic grain size of ~300–400 Å and local arrangement of grains along [001] and [010] directions. A complex contrast pattern results from superposition of compositional ordering and of morphological transformation effects. The height of the corrugation is about 20 Å as is determined by cross-section TEM studies. We note that complex lateral structures have been previously revealed in TEM studies of (In,Ga,As)P epilayers.²

The TEM image of sample B* [Fig. 1(d)] illustrates the influence of growth conditions on the resulting (In,Ga)As arrangement. Although the average thickness of the $\text{In}_x\text{Ga}_{1-x}\text{As}$ and the average composition are similar to that of sample B, the dots are larger and are much better separated in the B* case. The dots have a size of about 250–300 Å and are arranged in a lattice with main axes forming an angle of ~75°. The large size of the QDs results in a luminescence peak wavelength of 1.31 μm at 300 K. Thus, the maximum of PL emission is shifted by ~120 meV towards lower energies with respect to the emission from sample B having the same average indium composition (31%) and even slightly larger average width. A strong impact of the deposition mode on the PL peak energy for even lower composition $\text{In}_x\text{Ga}_{1-x}\text{As}$ insertions was already demonstrated in Ref. 10. No dislocations or large clusters were revealed over the macroscopic distances in all the four cases (samples A, B, B*, and C). Higher indium compositions result for the same average thickness of the deposits in the formation of dense networks of mesoscopic plastically relaxed clusters.

The laterally modulated structures (LMS) discussed here are used as active regions of strained (In,Ga,Al)As lasers grown on Si-doped GaAs(100) substrates. Some luminescence and lasing properties of such lasers grown by MBE are discussed in Ref. 14.

In this work, we concentrate on electroluminescence polarization, lasing energies, gain saturation effects, and on high power operation of MOCVD grown (In,Ga,Al)As lasers

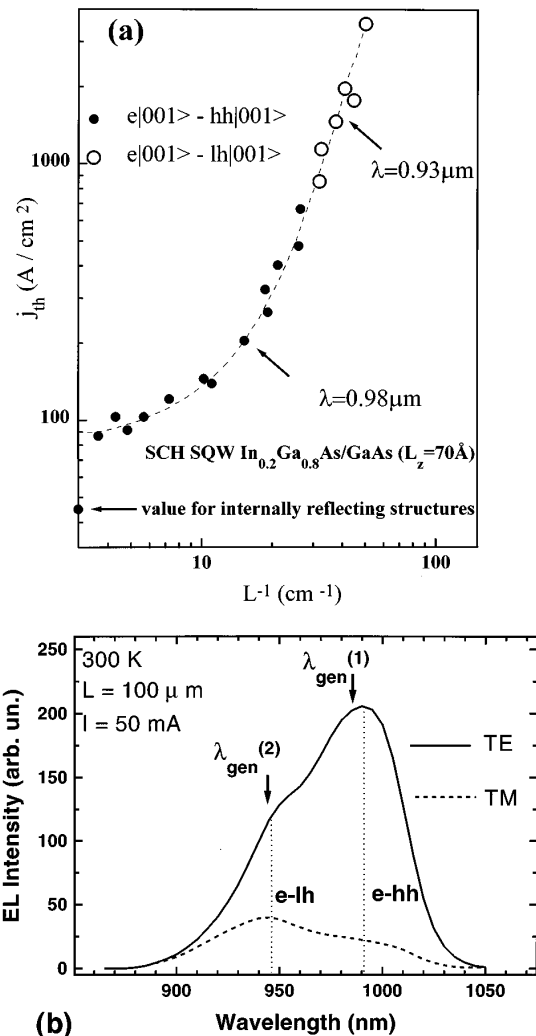


FIG. 2. (a) Threshold current density vs reverse cavity length for the laser structure with laterally modulated $\text{In}_x\text{Ga}_{1-x}\text{As}$ active region. (b) Polarized electroluminescence spectra of the laser.

with LMS in the active regions. The laser extensively studied in this work has an $\text{In}_x\text{Ga}_{1-x}\text{As}$ active region deposited under the same growth conditions as used for sample C. The laser geometry represents a conventional GaAs–(Al,Ga)As graded index separate confinement heterostructure with $\text{In}_x\text{Ga}_{1-x}\text{As}$ active region.¹⁵

In Fig. 2(a), we show the dependence of the threshold current density on the reverse cavity length for lasers fabricated in a shallow mesa stripe geometry. J_{th} measured for long cavity lengths is ~85 A cm^{-2} . The J_{th} values for the four side cleaved samples where external losses are minor, macroscopic nonuniformities of the active region do not play a significant role, and the carrier spreading out of the stripe region¹⁵ is absent, show much lower threshold current densities (43–48 A cm^{-2}), which are comparable to the best reported results for lasers in this wavelength range.^{16–18}

For cavity lengths smaller than 200 μm, the gain due to electron to heavy hole transition ($e|001\rangle-hh|001\rangle$) at 0.98 μm saturates and the lasing spectrum is dominated by a transition at ~0.93–0.95 μm. The energy difference between these two transitions corresponds to ~40–68 meV. According to the average composition and width of the $\text{In}_x\text{Ga}_{1-x}\text{As}$ layer, this corresponds to a transition between

the $\text{In}_x\text{Ga}_{1-x}\text{As}$ conduction band and localized light hole states ($e|001\rangle - |h|001\rangle$), as the lasing involving the second electron level (resonant to the GaAs conduction band) should occur at significantly shorter wavelength (~ 915 nm).

This conclusion is further confirmed by the polarization analysis of the electroluminescence. In Fig. 2(b), we show TE and TM polarized components of the electroluminescence below threshold. Two peaks can be clearly distinguished. One at $0.98 \mu\text{m}$ has a pronounced TE polarization and the other at $\sim 0.94 \mu\text{m}$ is more pronounced in the TM polarization. Both peaks demonstrate significant admixture of the opposite polarization. This can be expected for transitions involving light holes, where transition probabilities in a quantum well (QW) case are $2/3$ and $1/3$ for TM and TE components, respectively. In contrast, significant depolarization of the heavy-hole-related electroluminescence which has to be 100% TE polarized in a strained QW case, indicates violation of selection rules. This can be well explained by in-plane strain and by lateral confinement effect due to the LMS of the active region. Despite the $e|001\rangle - |h|001\rangle$ transition is more pronounced in the TM polarization the *total* gain is always higher for the TE mode, due to the strong gain of the TE-polarized continuum of the heavy-hole related states. The lasing at $e|001\rangle - |h|001\rangle$ energy, thus, also occurs in the TE polarization, and is caused by the TE contribution on the light-hole related transition. We note, that lasing involving light hole state in the continuum of electron to heavy-hole transition has not been reported for GaAs-AlGaAs quantum wells and is, probably, specific to laterally modulated structures.

Internal efficiency (η_i) of the laser estimated from the slope of differential efficiency (η_{diff}) versus inverse cavity lengths is 95% and the internal losses (α_i) are about 2.5 cm^{-1} . Maximum (η_{diff}) approaches 90%. Continuous wave (cw) operation with an output power of 3 W is realized at room temperature at a current of 5.5 A for lasers with dielectric mirrors with reflectivities of 10% and 90% (cavity length is $950 \mu\text{m}$). Maximum conversion efficiency of 52% is obtained. The lasers demonstrate cw operation lifetime of 1000 h at output light power of 1 W. In pulsed mode (200 ns), a maximum power of 15 W is realized at 20 A. Even better values are reported now for InGaAs/InGaP/GaAs lasers,¹⁹ however our data demonstrates for the first time that structures with LMS are also suitable for high power operation.

To conclude, our results demonstrate the formation of laterally modulated low indium composition $\text{In}_x\text{Ga}_{1-x}\text{As}$ structures and the possibility to realize injection lasers using them in the active region. Further progress in this area is related to the possibility to realize *efficient* 3D confinement by proper optimization of growth conditions, growth mode, and postgrowth annealing. Additional lateral confinement can lead to a strong increase in material gain and in better temperature stability of the laser. Complete localization of nonequilibrium carriers in all three dimensions presents new opportunities to solve many engineering problems in modern devices. For example, overheating of laser facets due to surface recombination, spreading of carriers out of the active regions, nonradiative recombination of mesa sidewalls, etc., can be avoided. LMS can extend the spectral range of (In-

GaAl)As lasers on GaAs substrates, and will, probably, permit lasing even in matrices containing high density of defects [e.g., in (InGaAl)As lasers on silicon substrates].

This work is supported by VW Stiftung, INTAS Grant No. 94-1028, Russian Foundation of Basic Research and by DFG in the framework of Sfb 296. One author (N.N.L.) is grateful to the Humboldt Foundation.

¹Y. Arakawa and H. Sakaki, Appl. Phys. Lett. **40**, 939 (1982); M. Asada, M. Miyamoto, and Y. Suematsu, IEEE J. Quantum Electron. **QE-22**, 1915 (1986).

²T. L. McDevitt, S. Mahajan, D. E. Laughlin, W. A. Bonner, and V. G. Keramidis, Phys. Rev. B **45**, 6614 (1992).

³L. Goldstein, F. Glas, J. Y. Marzin, M. N. Charasse, and G. Le Roux, Appl. Phys. Lett. **47**, 1099 (1985); S. Guha, A. Madhukar, and K. C. Rajkumar, Appl. Phys. Lett. **57**, 2110 (1990).

⁴D. Leonard, M. Krishnamurthy, C. M. Reeves, S. P. Denbaars, and P. M. Petroff, Appl. Phys. Lett. **63**, 3203 (1993); J. M. Moison, F. Houzay, F. Barthe, L. Leprince, E. Andre, and O. Vatel, Appl. Phys. Lett. **64**, 196 (1994).

⁵N. N. Ledentsov, M. Grundmann, N. Kirstaedter, J. Christen, R. Heitz, J. Böhrer, F. Heinrichsdorff, D. Bimberg, S. S. Ruvimov, P. Werner, U. Richter, U. Gösele, J. Heydenreich, V. M. Ustinov, A. Yu. Egorov, M. V. Maximov, P. S. Kop'ev, and Zh. I. Alferov, *Proceedings of the 22nd International Conference on the Physics of Semiconductors, Vancouver, Canada, 1994*, edited by D. J. Lockwood (World Scientific, Singapore, 1995), Vol. 3, p. 1855.

⁶V. A. Shchukin, N. N. Ledentsov, P. S. Kop'ev, and D. Bimberg, Phys. Rev. Lett. **75**, 4043 (1995); D. Bimberg, N. N. Ledentsov, M. Grundmann, N. Kirstaedter, O. G. Schmidt, M. H. Mao, V. M. Ustinov, A. Yu. Egorov, A. E. Zhukov, P. S. Kop'ev, Zh. I. Alferov, S. S. Ruvimov, U. Gösele, and J. Heydenreich, Phys. Status Solidi B **194**, 159 (1996).

⁷N. Kirstaedter, N. N. Ledentsov, M. Grundmann, D. Bimberg, U. Richter, S. S. Ruvimov, P. Werner, J. Heydenreich, V. M. Ustinov, M. V. Maximov, P. S. Kop'ev, and Zh. I. Alferov, Electron. Lett. **30**, 1416 (1994).

⁸Zh. I. Alferov, N. A. Bert, A. Yu. Egorov, A. E. Zhukov, P. S. Kop'ev, A. O. Kosogov, I. L. Krestnikov, N. N. Ledentsov, A. V. Lunev, M. V. Maximov, A. V. Sakharov, V. M. Ustinov, A. F. Tsatsulnikov, Yu. M. Shernyakov, and D. Bimberg, Fiz. Tekh. Poluprovodn. **30**, 351 (1996); Semiconductors **30**, 194 (1996).

⁹N. N. Ledentsov, V. A. Shchukin, M. Grundmann, N. Kirstaedter, J. Böhrer, O. Schmidt, D. Bimberg, V. M. Ustinov, A. Yu. Egorov, A. E. Zhukov, P. S. Kop'ev, S. V. Zaitsev, N. Yu. Gordeev, Zh. I. Alferov, A. I. Borovkov, A. O. Kosogov, S. S. Ruvimov, P. Werner, U. Gösele, and J. Heydenreich, Phys. Rev. B **54**, 8743 (1996).

¹⁰P. D. Wang, N. N. Ledentsov, C. M. Sotomayor Torres, P. S. Kop'ev, and V. M. Ustinov, Appl. Phys. Lett. **64**, 1526 (1994).

¹¹G. E. Tsyrlin, A. O. Golubok, and S. Ya. Tipisev, Fiz. Tekh. Poluprovodn. **29**, 1697 (1995) [Semiconductors **29**, 885 (1995)].

¹²R. P. Mirin, J. P. Ibbetson, K. Nishi, A. C. Gossard, and J. E. Bowers, Appl. Phys. Lett. **67**, 3795 (1995).

¹³S. S. Ruvimov, P. Werner, K. Scheerschmidt, U. Gösele, J. Heydenreich, U. Richter, N. N. Ledentsov, M. Grundmann, D. Bimberg, V. M. Ustinov, A. Yu. Egorov, P. S. Kop'ev, and Zh. I. Alferov, Phys. Rev. B **51**, 14 766 (1995); F. Heinrichsdorff, A. Krost, M. Grundmann, D. Bimberg, A. Kosogov, and P. Werner, Appl. Phys. Lett. **68**, 3284 (1996).

¹⁴N. N. Ledentsov, M. Grundmann, N. Kirstaedter, O. Schmidt, R. Heitz, J. Böhrer, D. Bimberg, V. M. Ustinov, V. A. Shchukin, P. S. Kop'ev, Zh. I. Alferov, S. S. Ruvimov, A. O. Kosogov, P. Werner, U. Richter, U. Gösele, and J. Heydenreich, Solid-State Electron. **40**, 785 (1996).

¹⁵P. S. Kop'ev and N. N. Ledentsov, Fiz. Tekh. Poluprovodn. **24**, 1691 (1990) [Sov. Phys. Semicond. **24**, 1058 (1990)].

¹⁶H. K. Choi and C. A. Wang, Appl. Phys. Lett. **57**, 321 (1990).

¹⁷Zh. I. Alferov, A. M. Vasiliev, S. V. Ivanov, P. S. Kop'ev, N. N. Ledentsov, B. Ya. Meltser, and V. M. Ustinov, Pis'ma Zh. Tekn. Fiz. **14**, 1803 (1988) [Sov. Tech. Phys. Lett. **14**, 782 (1988)].

¹⁸Zh. I. Alferov, S. V. Ivanov, P. S. Kop'ev, N. N. Ledentsov, M. E. Lutsenko, M. I. Nemenov, B. Ya. Meltser, V. M. Ustinov, and S. V. Shaposhnikov, Fiz. Tekh. Poluprovodn. **24**, 152 (1990) [Sov. Phys. Semicond. **24**, 92 (1990)].

¹⁹L. J. Mawst, A. Bhattacharya, L. Lopez, D. Boetz, D. Z. Garbuzov, L. DeMarco, J. C. Connolly, M. Jansen, F. Fang, and R. F. Nabiev, Appl. Phys. Lett. **69**, 1532 (1996).